J Comp Physiol A (2000) 186: 119–128 

ORIGINAL PAPER

M. Blum · T. Labhart

# Photoreceptor visual fields, ommatidial array, and receptor axon projections in the polarisation-sensitive dorsal rim area of the cricket compound eye

Accepted: 4 November 1999

**Abstract** We made intracellular recordings from the photoreceptors of the polarisation-sensitive dorsal rim area of the cricket compound eye combined with dye marking. By measuring visual field sizes and optical axes in different parts of the dorsal rim area, we assessed the optical properties of the ommatidia. Due to the large angular sensitivities (median about 20°) and the high sampling frequency (about 1 per degree), the visual fields overlap extensively, such that a given portion of the sky is viewed simultaneously by a large number of ommatidia. By comparing the dye markings in the retina and in the optic lobe, the axon projections of the retinula cells were examined. Receptors R1, R2, R5 and R6 project to the lamina, whereas R7 projects to the medulla. The microvilli orientation of the two projection types differ by 90° indicating the two analyser channels that give antagonistic input to polarisation-sensitive interneurons. Using the retinal marking pattern as an indicator for the quality of the intracellular recordings, the polarisation sensitivity of the photoreceptors was re-examined. The polarisation sensitivity of recordings from dye-coupled cells was much lower (median: 4.5) than that of recordings in which only one cell was marked (median: 9.8), indicating that artefactual electrical coupling between photoreceptors can significantly deteriorate polarisation sensitivity. The physiological value of polarisation sensitivity in the cricket dorsal rim area is thus typically about 10.

**Key words** Polarisation vision · Photoreceptors · Compound eye · Optic lobe · *Gryllus campestris*

**Abbreviations** *DRA* dorsal rim area · *LVF* long visual fibre · *SVF* short visual fibre · *PS* polarisation sensitivity

M. Blum · T. Labhart (✉)
Zoologisches Institut der Universität, Winterthurerstrasse 190, CH-8057 Zürich, Switzerland
e-mail: labhart@zool.unizh.ch
Tel.: +41-1-635-4832; Fax: + 41-1-635-5716

## Introduction

Apart from the sun, skylight polarisation offers insects a useful reference system in visual compass orientation or course control. Crickets (*Gryllus* sp.) belong to those insects in which the mechanisms of polarisation vision have been studied most thoroughly both at the photoreceptor and interneuron level (e.g. Brunner and Labhart 1987; Burghause 1979; Herzmann and Labhart 1989; Labhart 1988, 1996; Labhart et al. 1984; Nilsson et al. 1987; Zufall et al. 1989; for a review see Labhart and Petzold 1993). At the retina level, many of the relevant anatomical, optical and electrophysiological properties of the polarisation-sensitive photoreceptors have been described in detail (e.g. Burghause 1979; Nilsson et al. 1987; Zufall et al. 1989; for a review see Labhart and Petzold 1993). As in other insects (reviewed by Labhart and Meyer 1999), polarisation vision in crickets is mediated by a comparatively small group of anatomically and physiologically specialised ommatidia situated at the dorsal rim of the compound eye, an eye region termed the dorsal rim area (DRA).

When observing the DRA of an intact cricket eye under a dissecting microscope, two remarkable features attract attention. First, the DRA has a pale, whitish appearance, in contrast to the rest of the eye, which is brown. Histological studies revealed that this is because the DRA is devoid of screening pigment (Burghause 1979), and as a consequence the visual fields of DRA ommatidia are very large (Labhart et al. 1984). Second, compared to the rest of the eye, the DRA appears curiously flat. The virtually absent curvature suggests only little or no deviation between the optical axes of DRA ommatidia. In this case, all DRA ommatidia would receive light from roughly the same part of the sky, especially when the large visual fields are taken into account. This thesis could not be tested so far since the DRA does not exhibit a pseudopupil due to the missing screening pigment. The cricket DRA is therefore resistant to the elegant pseudopupil approach usually

employed for measuring optical axes in insect eyes (compare e.g. Beersma et al. 1977; Zollikofer et al. 1995).

Apart from the optical projection of DRA photoreceptors to the sky, the anatomical projections of the receptor axons to the optic lobe are also uncertain: the findings of two previous studies of the axon projections are controversial (Jud and Labhart 1985; Zufall et al. 1989), and the connectivity pattern between photoreceptor terminals and polarisation-sensitive interneurons in the medulla (Labhart 1988) remains elusive so far, in spite of several experimental attempts (J. Petzold, unpublished observations).

The present study addresses two main questions. First, we assess the optical properties of the DRA by measuring the visual field sizes and the optical axes of ommatidia in different parts of the DRA. Second, we examine the axon projections of DRA photoreceptors to the optic lobe. The method of choice to solve both problems with one and the same approach was to record intracellularly from photoreceptors in different parts of the DRA, measure their optical axes and visual fields, and finally mark the photoreceptors with dye. In this way, the optical axis of a photoreceptor could be related to its position in the DRA. Each cell marking in the retina was further studied under high magnification to determine which cell within an ommatidium was stained. This information allowed us to assign the stained receptor axons in the optic lobe to specific receptor somata in the retinula. This approach also enabled us to critically re-examine polarisation sensitivity of DRA photoreceptors by comparing data associated with single-cell markings with those obtained from dye-coupled cells. Our findings help understand some of the characteristic physiological properties of the polarisation-sensitive neurons found in the cricket's optic (Labhart 1988).

## Materials and methods

### Animals

Adult field crickets, *Gryllus campestris*, were used for the experiments. They were laboratory-bred F1 offspring of crickets collected in the field. The crickets were kept and bred under long-day conditions (L/D = 14/10 h) at 26 °C or 20 °C, and 60% relative humidity. Lighting was provided by Osram L20W/10S daylight lamps.

### Stimulation

Light was supplied by a 900 W xenon arc lamp. Interference filters were used to generate quasi-monochromatic light, intensity was controlled by a neutral-density wedge, and an electromagnetic shutter provided temporal control of the stimulus. The light was focused into a flexible light guide the other end of which was mounted on a perimeter device. For measuring responses to polarised light, a linear polariser (HNP'B, Polaroid) was inserted in front of the exit end of the light guide. The stimulus had a diameter of 1.0° and a wavelength of 440 nm (except for identifying the spectral receptor type) and maximal intensity was $1.7 \times 10^{13}$ $Q$ $s^{-1}$ $cm^{-2}$. For stimulation with flashes, 100 ms light pulses were used and the interstimulus interval was 5 s (visual field) or 10 s (polarisation sensitivity).

The *spectral type* of a photoreceptor was identified by four successive monochromatic flashes (adjusted to equal quanta), i.e. 341 nm, 440 nm, 520 nm and 341 nm again. *Angular sensitivities* were measured along two axes approximately parallel (*x*-axis) and orthogonal (*y*-axis) to the long axis of the dorsal rim area using series of flashes at intervals of 4°. *Polarisation sensitivity* (PS) was measured by an 18° e-vector series of flashes covering 360°. Interspersed between these measurements $R/\log I$ *functions* were taken using 0.3 log intensity series of flashes. To assess the e-vector of maximal sensitivity $\Phi_{max}$, the photoreceptors were stimulated with continuous light with the polariser rotating constantly from 0° to 360° and back with an angular velocity of ca. 80° $s^{-1}$. Two methods were used to determine the optical axis of a receptor. (1) A "searchlight" consisting of a tiny incandescent light bulb was moved manually within the visual field of a photoreceptor and the position of maximal receptor response was noted. (2) The maxima of the *x*- and *y*-angular sensitivity functions were determined.

### Preparation, recording and dye labelling

Crickets were waxed to a stage, their head was centred in the perimeter and oriented for suitable electrode approach. A small piece of cornea of the right eye was cut away with a razor-blade fragment as far away from the dorsal rim area as possible. The opening was immediately sealed with a thin layer of Vaseline using a warm heating coil. Borosilicate-glass micropipettes filled with 4% Neurobiotin (Vector Laboratories) in 2 $mol \cdot l^{-1}$ KCl were introduced into the retina through this opening and advanced to the dorsal rim retina. Intracellular signals from photoreceptors were measured using a high-impedance electrometer (M707, World Precision Instruments) and monitored with an oscilloscope. Cell responses, polariser orientation and shutter state were recorded on a DAT recorder (DTR 1800, Bio-Logic). After the electrophysiological experiments, the photoreceptors were iontophoretically marked with Neurobiotin using 1 to 3 nA depolarizing d.c. current for 10–20 min.

### Experimental protocol

After impaling a photoreceptor, its spectral class was checked with flashes at three wavelengths corresponding to the maximal sensitivities of the three spectral types in the cricket's compound eye. Blue receptors, which are present in the dorsal rim area only (Labhart et al. 1984), were further tested by first measuring the optical axis with the searchlight method (this stimulus position was maintained for all further measurements except for angular sensitivity). Then, the angular sensitivities in the *x*- and *y*-axis were measured with the two axes intersecting in the optical axis obtained with the searchlight, and subsequently PS was tested. Interspersed between these measurements, $R/\log I$ functions were taken. Finally, the e-vector response was recorded with the rotating polariser for assessing $\Phi_{max}$. After these tests the photoreceptor was marked with Neurobiotin. A final test with the rotating e-vector served to confirm that the $\Phi_{max}$ orientation was unchanged after iontophoresis. In each eye, two or three photoreceptors in different parts of the dorsal rim area were tested and marked in this way. After removing the cricket from the setup, the pseudopupils of the dorsal eye part of the two eyes (next to the dorsal rim area) were compared under axially incident light to check for possible shifts of the optical axes due to the preparation procedure.

### Evaluation of electrophysiological data

*Angular* and *polarisation sensitivity functions* were calculated from the response functions and the $R/\log I$ functions. *Optical axes* were defined by the coordinates of maximal sensitivity in the *x*- and *y*-angular sensitivity functions. The perimeter coordinates were

converted to values related to the cricket's natural head position (Labhart et al. 1984). *Acceptance angles* are given by the width of the angular sensitivity functions at the 50% sensitivity level. Since the stimulus did not move on an exact great circle in most of the *x*-angular sensitivity measurements, the perimeter readings had to be corrected. No acceptance angles were determined for photoreceptors in which the optical axis obtained with the searchlight deviated significantly from the optical axis defined by the angular sensitivity functions: criterion was at least 80% sensitivity at the former position in both the *x*- and the *y*-angular sensitivity functions (deviation mostly $< 4°$, in a few cases 6°).

PS is defined as the ratio between maximal and minimal sensitivity to the e-vector of polarised light. $\Phi_{max}$ was determined from the photoreceptor's response to the rotating e-vector. Smoothed traces were displayed on a computer screen and $\Phi_{max}$ was determined by aligning a measuring cursor with the response maxima. At least two traces obtained with each sense of e-vector rotation were evaluated and the $\Phi_{max}$ values were averaged, thus eliminating effects of response delay. $\Phi_{max}$ values are represented graphically (Fig. 2b) in a zenithal projection of the celestial hemisphere at their respective positions of optical axis (searchlight values). There, they are represented as bars oriented with reference to the respective meridians (see Fig. 2a in Schwind and Horváth 1993).

### Histology of intracellular dye markings

The cricket head was immersed in fixative and the eye including the optic lobe was removed. After cutting open the ventral part of the eye, the preparation was fixed for 2 h at room temperature in 4% paraformaldehyde in 0.1 $mol \cdot l^{-1}$ phosphate buffer (pH 7.4). After rinsing the preparation in 0.1 $mol \cdot l^{-1}$ phosphate buffer overnight, it was rinsed in water for 10 min and dehydrated with 2,2-dimethoxypropane. To make the tissue more permeable to the dye complex (see below) it was treated with 100% ethanol (30 min.), rehydrated with an ethanol series, and immersed in 0.5 $mol \cdot l^{-1}$ NaCl in 0.1 $mol \cdot l^{-1}$ bicarbonate buffer (pH 8.2; $2 \times 10$ min.). To attach a fluorescence marker to the Neurobiotin, the tissue was incubated with a Texas Red/Avidin complex (Texas Red Avidin DCS, Vector Laboratories; 20 $\mu g\ ml^{-1}$) in 0.1 $mol \cdot l^{-1}$ bicarbonate buffer containing 0.1% Tween at 7 °C overnight. After rinsing with bicarbonate buffer and water, the preparation was dehydrated with 2,2-dimethoxypropane, immersed in acetone (30 min), acetone/Epon (2 h) and embedded in Epon 812 (1 h at 50 °C and overnight at 65 °C). Cross-sections (5 μm thick) through the retina of the dorsal rim area were made with glass knifes on an ultramicrotome (Om U3, Reichert). By maintaining this section plane for the optic lobe we obtained longitudinal sections with respect to the receptor axons. They were 16 μm thick and were made with a heated (68 °C) steel knife on a Reichert/Jung microtome.

### Evaluation of intracellular dye markings

The sections were viewed and drawn with a fluorescence microscope (Zeiss Axiophot) using a Rhodamin filter set. Maps of dorsal rim area cross-sections containing the orientations and positions of the ommatidia were drawn using a drawing tube, and the positions of dye-labelled ommatidia were marked. This was done by using phase-contrast and fluorescence microscopy in combination (Zeiss objective Ph2 40×/0.75) using a small drawing tube magnification. Labelled ommatidia were also drawn more strongly enlarged to record the position of the labelled photoreceptors within the ommatidia (Zeiss Ph2 40×/0.75 or 63×/1.40). To correct for differently sized eyes (number of dorsal rim ommatidia is about 530–680 as counted in eight eyes) ommatidial positions were entered in a template dorsal rim area having a normalised length of 1.0 representing the number of ommatidia in the long axis of the dorsal rim area. The photoreceptors within each ommatidium were numbered according to Burghause (1979). Axonal projections were drawn with a 40×/0.75 objective.

### Retrograde labelling of photoreceptors

Crickets were anaesthetised with $CO_2$ and a window was cut in the head capsule to expose the optic lobe. A small incision was made in the dorsal part of the optic lobe with micro-scissors, a tiny crystal of Fluoro Ruby (Molecular Probes) was inserted into the lesion, and the head capsule was sealed with Vaseline. After 2 h the eye including the optic lobe was removed, fixed in 4% paraformaldehyde in 50 $mmol \cdot l^{-1}$ cacodylate buffer (pH 7.4, 500 $mosmol\ l^{-1}$) at room temperature for 2 h, rinsed with 50 $mmol \cdot l^{-1}$ cacodylate buffer, dehydrated with an ethanol series and embedded in Epon 812 as above. Cross sections (5 μm thick) through the retina of the dorsal rim area were made, and viewed and photographed with the fluorescence microscope (see above).

## Results

### Visual fields

The DRA of the cricket eye is characterised by peculiar optics: the ommatidia are devoid of screening pigment and the outer surface of the corneal lenses is flat (Burghause 1979; Ukhanov et al. 1996). As previously demonstrated electrophysiologically, the degraded optics strongly extends the visual fields of DRA ommatidia and induces a high variability of visual field size (Labhart et al. 1984). The present study confirms these findings. Visual field sizes (half widths of angular sensitivity functions) ranged from 6° to 67° along the *x*-axis (parallel to the long axis of the DRA), and from 6° to 37° along the *y*-axis (orthogonal to the long axis of the DRA), with median values of 20° and 22°, respectively ($n = 19$). In very large visual fields, the half widths were larger along the *x*-axis than along the *y*-axis. The narrowest sensitivity functions (half-widths $\leq 10°$) correlated with cell markings in ommatidia positioned in the lateral third of the DRA, i.e. near to the border of the unspecialised eye part. These ommatidia do contain some screening pigment distally, i.e. in the primary pigment cells (Brunner and Labhart 1987), in contrast to the more medially positioned ommatidia, which are completely pigment-free (Burghause 1979; T. Labhart, unpublished observations).

### Topological relation between optical axes and retinal position

In a compound eye, there is an exact topological relation between points in space and position of ommatidia in the retina. Is this order conserved in the cricket DRA despite the coarse optics? As found by comparing optical axes and retinal positions of pairs of dye-marked photoreceptors, this seems to be true in principle. In 14 out of 16 pairs of receptor cells the antero-posterior order was the same for optical axis and retinal position, and just in two pairs involving especially large visual fields the order was slightly reversed (14 crickets studied). Representative data are given in Fig. 1A. On the left side of the figure, the retinal positions of the marked

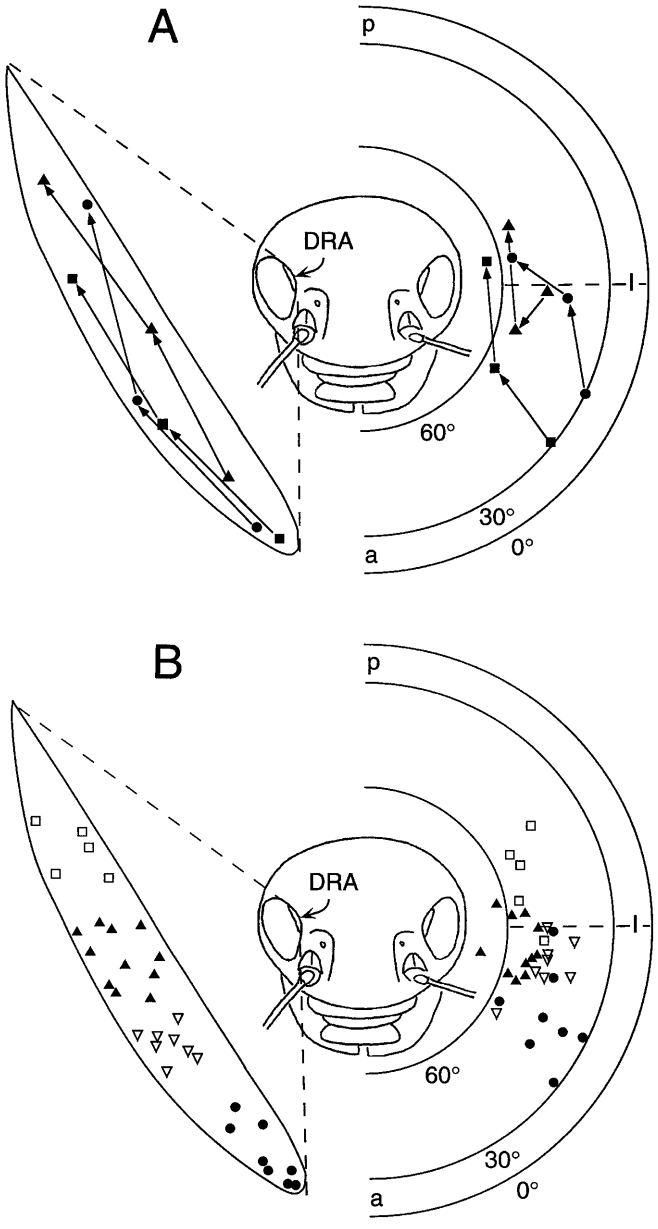


**Fig. 1A, B** Topological relation between retinal position and optical axis in photoreceptors of the dorsal rim area of the eye. The *left side* of graphs shows the positions of dye-marked photoreceptors in the retina (template of the dorsal rim area; see Materials and methods). On the *right side*, the corresponding optical axes are indicated on the celestial hemisphere. **A** Data from 3 crickets (see different symbols). The *arrows* connecting the symbols indicate the antero-posterior order in the retina. **B** Data from 14 crickets. The dye-marked photoreceptors are grouped according to their retinal positions (see different symbols). *a* anterior, *p* posterior, *l* left, *numbers* indicate elevation

photoreceptors were entered in a template of the cricket's right DRA, with the different symbols representing three different crickets (the template corrects for different eye sizes; see Materials and methods). On the right side, the corresponding optical axes are projected on the celestial hemisphere. Note that the optical axes of dorsal rim ommatidia are directed to the contralateral side (see also Labhart et al. 1984). In all but one of these examples, both optical axes and retinal positions change in the same sense (see arrows between data points). In Fig. 1B the retinal positions of the marked receptors of all 14 crickets are entered in the template DRA and grouped according to their positions with respect to the DRA long axis (see different symbols). For the optical axes, the order of those groups is maintained, confirming the findings based on the individual crickets; namely, the topological relation between space and retinal position is generally maintained along the long axis of the DRA, meaning that different parts of the DRA are directed to different parts of the sky.

To estimate the spatial sampling frequency (Snyder 1979) of the ommatidial array in the long axis of the DRA, the retinulae encountered along a straight line between two marked receptor cells were counted, and the angle between the optical axes was calculated. By dividing retinula count by angular distance, one arrives at a sampling frequency of slightly more than 1 per degree (average 1.15 per degree, range 0.9–1.4 per degree, $n = 7$). A comparison of this figure to the wide angular-sensitivity profiles of some 20° half-width shows that the visual fields of DRA ommatidia overlap extensively. The optical axes of the two middle groups of marked receptors are very close (see Fig. 1B); this may indicate that sampling frequency in the middle part of the DRA is higher than in the anterior and posterior section. Since no marking series were made orthogonal to the DRA long axis, the sampling frequency in this direction can only be estimated. By comparing the distribution of the optical axes (Fig. 1B) with the width of the DRA (number of retinulae, Fig. 2A), and considering some noise in the optical axis data, one arrives at a sampling frequency orthogonal to the DRA of at least ca. 0.4.

## Projections of receptor cell axons

The present study of axon projections of DRA photoreceptors was prompted by two previous, contradictory reports. Whereas Zufall et al. (1989) detected both fibres terminating in the lamina (short visual fibers, SVFs) and in the medulla (long visual fibres, LVFs), Jud and Labhart (1985) found that all DRA photoreceptors gave rise to LVFs. Unlike the previous authors, here we studied the anatomy of dye-marked receptors in both the optic lobe and the retina, which allowed us to assign axon projections to specific receptor somata in the retinula.

In cross-section, the rhabdoms of the ommatidia in the DRA have characteristic trapezoidal shapes (Fig. 2A inset). At a distal level, the five receptor cells R1, R2, R5, R6 and R7 form the rhabdom (Burghause 1979). Proximally, the short cell R8 also contributes to the rhabdom between R1 and R7. R3 and R4 do not form any microvilli. Burghause (1979) based the identification of receptor cells within the retinula (cell numbers) on the arrangement of the crystalline cone processes that run between the receptor somata. As two types of crystalline cone arrangement occur in the eye, cell numbering is

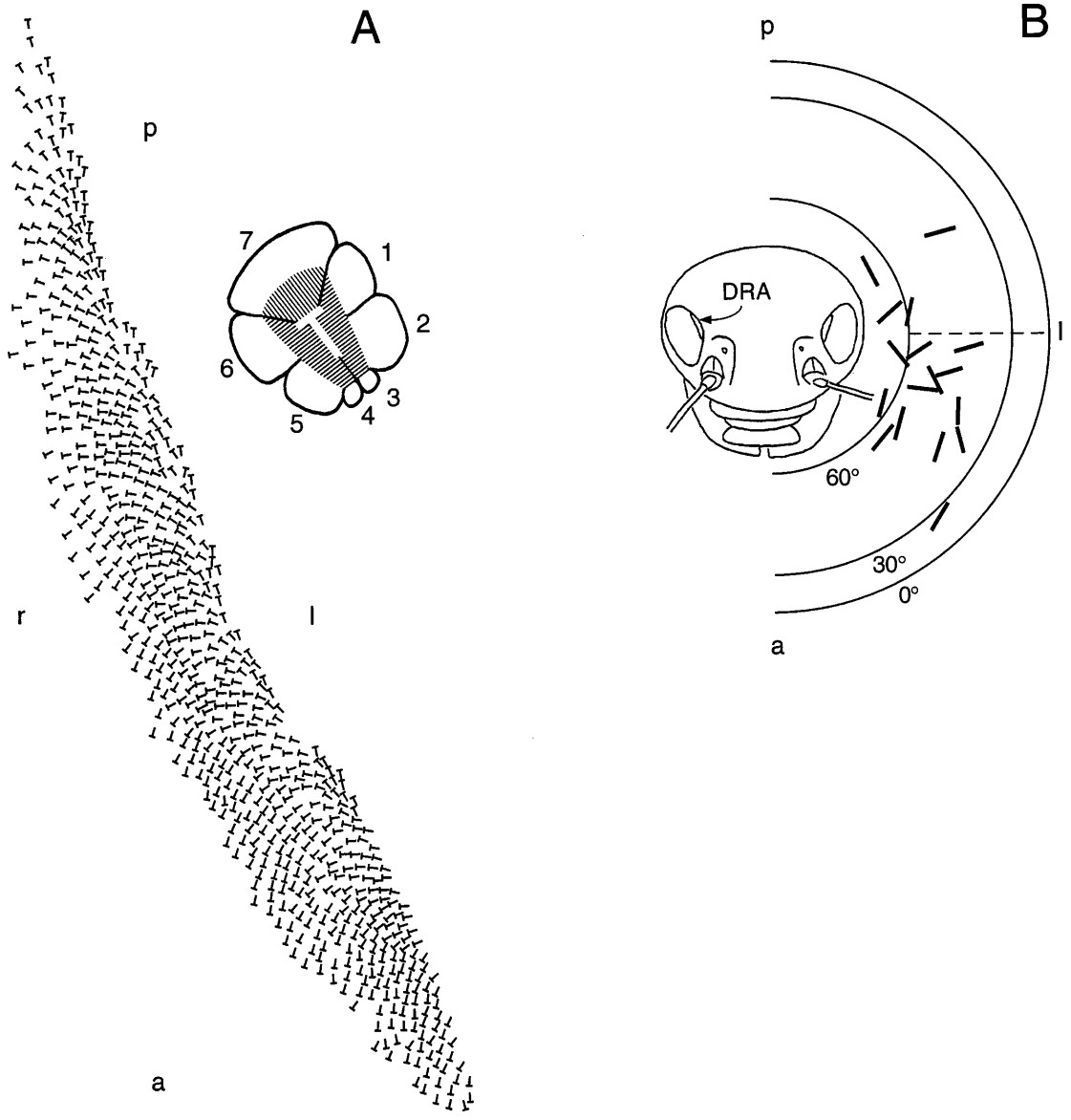


**Fig. 2** **A** Distribution and orientation of retinulae in the dorsal rim area of the eye. Schematic drawing of a cross-section through the dorsal rim area of a right eye. The Ts indicate the position and orientation of the retinulae. The *inset* shows an enlarged cross-section through an ommatidium with the *white inscribed T* defining the Ts used in the figure. The short, proximal cell R8 is not visible in this distal section. **B** E-vector of maximal sensitivity $\Phi_{max}$ of dorsal rim photoreceptors R7. $\Phi_{max}$ (*bars*) is indicated on the celestial hemisphere (for conventions, see Materials and methods) with the position of the centres of the bars indicating the optical axes of the cells. For recordings from cells other than R7 the $\Phi_{max}$ values were corrected by 90°. The bars thus indicate the orientation in space of the analyser channel represented by R7. *a* anterior, *p* posterior, *l* left, *r* right

either clockwise or anti-clockwise. In light-microscopical sections, R7 is easily recognised by its position at the base of the trapezoid formed by the rhabdom. However, our light-microscope inspection did not reveal the crystalline cone projections or allow reliable identification of unmarked R8 cells. We were thus unable to discriminate R1 from R6 (the cells flanking R7), and R2 from R5 (the cells forming the narrow end of the rhabdom) in our retinal cross-sections.

Our first approach to study axon projections was to mark the photoreceptors in the retina by intracellular injection of dye. In about half of our markings, more than one receptor cell of an ommatidium contained dye or cells in more than one ommatidium were stained. In these cases, it was impossible to assign projection types to receptor somata. Regarding single-cell markings only, we found that all stained R7 somata projected to the medulla ($n = 10$). All R1/6 cells ($n = 4$) and a R2/5 cell ($n = 1$) terminated in the lamina (for examples see Fig. 3). We did not succeed in marking cell R8. Multiple cell markings did not contain more than one LVF per ommatidium. Thus, we tentatively concluded that R7 has a LVF, whereas R1, R2, R5 and R6 have SVFs. This thesis was tested by a second approach, which was to stain the photoreceptors by the retrograde labelling technique. When dye was applied to the lamina, all

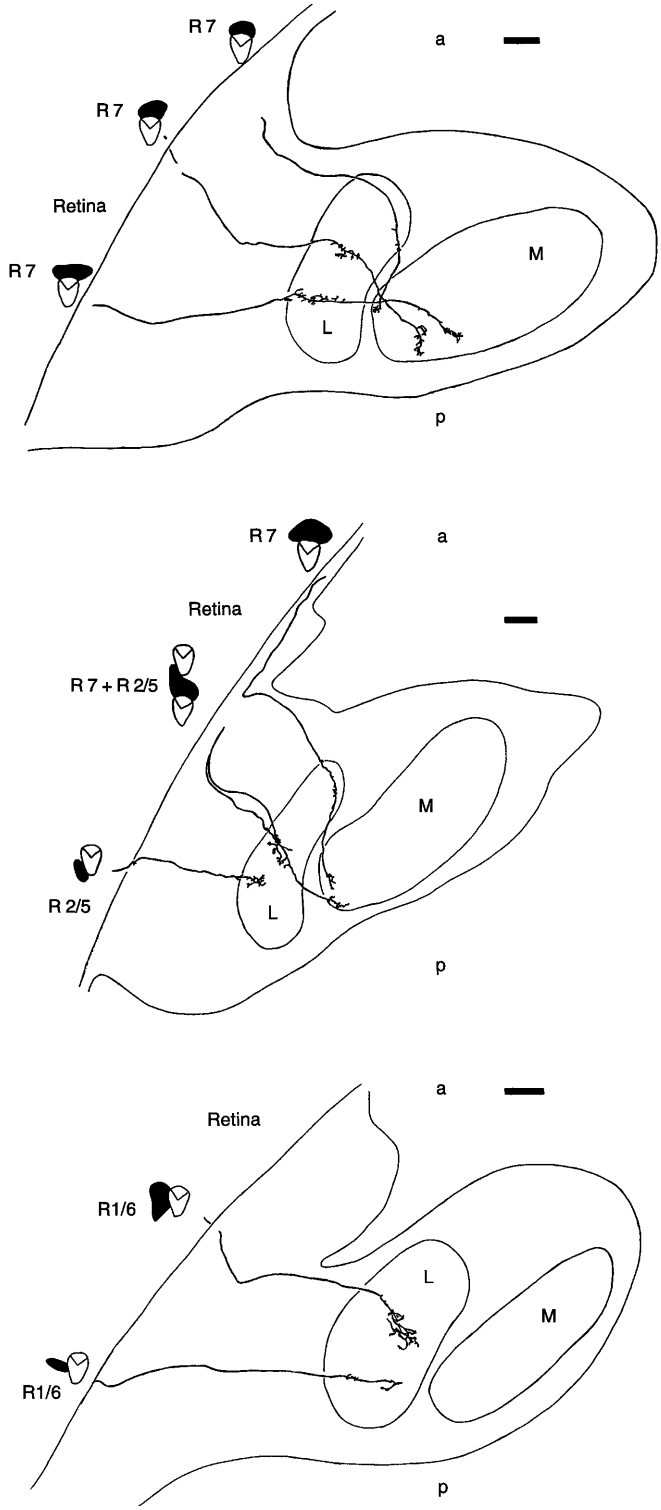


**Fig. 3** Projections of photoreceptor axons to the optic lobe. Results of intracellular dye-markings in three crickets are shown. In each cricket, dye was injected intracellularly at two or three positions of the dorsal rim area. The *upper left* of the drawings shows the staining pattern as observed in cross-sections through the retinulae. Axon projections were drawn from horizontal sections through the optic lobe. *L* lamina, *M* medulla, *a* anterior, *p* posterior, *scale bar* (for axon drawings) 50 μm

receptor somata were marked in retinal cross sections. When dye was applied to the medulla, the somata of R7 and R8 were marked. These data are in accordance with our previous conclusions. In addition, R8 seems to have a LVF (but see Discussion). Thus, for the large cells we can safely conclude that receptor R7 has a LVF projecting to the medulla, whereas receptors R1, R2, R5 and R6 have SVFs terminating in the lamina.

Although in our intracellular dye markings the discrimination between SVFs and LVFs was unequivocal, further categories based on branching patterns could not be made (compare also Zufall et al. 1989). The observed branching patterns were quite variable, either naturally or due to variability in the staining process. Note, however, that the axons of R7 branch both in the lamina and the medulla and, like in other eye parts, are subject to an antero-posterior chiasma.

## Polarisation sensitivity

PS varied widely between recordings. PS values ranged from 1.6 to 29 with a median of 6.2 ($n = 40$; Fig. 4A).

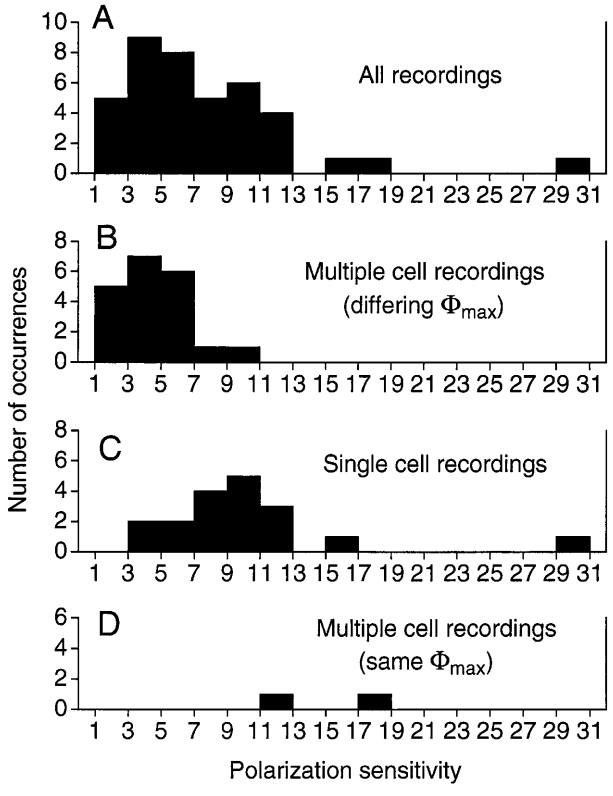


**Fig. 4A–D** Polarisation sensitivity (PS) of photoreceptors in the dorsal rim area of the eye. Comparison between single- and multiple-cell recordings (classification based on intracellular staining pattern). **A** All recordings (median PS = 6.2, $n = 40$). **B** Multiple-cell recordings in which the microvilli orientations of the dye-coupled cells differed by 90° (median PS = 4.5, $n = 20$). **C** Single-cell recordings (median PS = 9.8, $n = 18$). **D** Multiple-cell recordings in which the microvilli orientation of the dye-coupled cells was the same (PS = 11.7 and 18.2, $n = 2$)

What could be the reason for this large scatter? PS can be strongly affected by electrical coupling between photoreceptors when coupling occurs between cells that are tuned to different e-vectors. In our study, we could discriminate between single- and multiple-cell recordings by using dye-coupling as an indicator for electrical coupling. We could also determine whether coupling was between cells tuned to the same or to a 90° different e-vector, in the following way: in microvillar photoreceptors, the e-vector of maximal sensitivity $\Phi_{max}$ is indicated by the orientation of the microvilli (e.g. Goldsmith and Wehner 1977; Hardie 1984; Kirschfeld 1969). The microvilli orientation, in turn, can be read from a photoreceptor's position in the ommatidium with the light microscope (see Fig. 2A inset).

PS of multiple cell recordings involving different $\Phi_{max}$ ranged from 1.6 to 10.8 with a median of 4.5 ($n = 20$; Fig. 4B). In single-cell recordings, PS values were generally higher, ranging from 4.6 to 29 with a median of 9.8 ($n = 18$; Fig. 4C). Thus, the PS values of single- and multiple-cell recordings differ markedly ($P < 0.0001$, Mann-Whitney $U$-test). PS was also high (11.7 and 18.2) in the two cases in which coupling was between cells having the same $\Phi_{max}$ (Fig. 4D). We found no significant difference in PS between single cell recordings from R7 (range 4.6–29, median 10.8, $n = 11$) and from R1/6 or R 2/5 (range 5.5–15.3, median 8.5, $n = 7$; $P = 0.5$).

## Discussion

### Optical properties of the dorsal rim area

With half-widths of some 20° (median), the visual fields of DRA ommatidia are much wider than the visual fields of ommatidia in the unspecialised, dorsal part of the eye (6°; Labhart et al. 1984). There are several factors that widen the visual fields in the DRA. (1) The ommatidia lack screening pigment either completely or within the receptor cells, thus abandoning optical separation (Brunner and Labhart 1987; Burghause 1979). (2) The rhabdoms of the DRA are much wider than in the rest of the eye (Burghause 1979). (3) Compared with the lenses of regular ommatidia, the lens curvature is altered in such a way that the ommatidia become under-focused (Ukhanov et al. 1996).

The strong variability of visual field size, as found both in the present and in our earlier study of the cricket DRA (Labhart et al. 1984), is unusual. Could this variability arise due to variable degrees of damage inflicted to the optics while preparing the eye for recording or during the experiments by the electrode tip? For the following reasons we think that the strong variability of visual field size is not an artefact. First, there is an inherent variability of the optical properties of DRA ommatidia both regarding the content of screening pigment (Brunner and Labhart 1987; Burghause 1979), and optical quality and focal distance of the facet lenses (Ukhanov et al. 1996). Second, in both the present and our previous study (Labhart et al. 1984), we found the pseudopupil of the unspecialised eye part next to the DRA undisturbed, and control recordings from this area revealed small visual fields.

At least along its long axis, the DRA has a sampling frequency of about 1 per degree, which is quite high by insect standards. For comparison, we measured spatial resolution in the unspecialised eye part next to the DRA (parallel to the DRA long axis) using the pseudopupil method, and found a sampling frequency of 0.4–0.5 per degree. Thus, the unpigmented DRA has a higher sampling frequency than the dorsal part of the eye that is composed of regular, pigmented ommatidia. This may seem paradoxical at first glance.

Our data show that a topological relation between retinal position and optical axis does exist in the DRA, at least in the DRA long axis, meaning that ommatidia in the anterior part of the DRA are directed to the anterior part of the DRA's visual field, whereas ommatidia in the posterior part of the DRA are directed to the posterior part of the visual field (see Fig. 1). However, compared to the size of the visual fields, the divergence between the optical axes is so small that the ommatidia within a given section of the DRA receive light from practically the same area of the sky. Evidently, the high sampling frequency does not serve to increase spatial resolution in the DRA but to increase overlap of the visual fields, an effect that is boosted by the extreme width of the visual fields.

What could be functional significance of the peculiar, rather degraded optics in the DRA? Before answering this question, we must consider some background details. The e-vector information collected by the polarisation-sensitive photoreceptors of the DRA is processed by so-called POL-neurons (Labhart 1988). In these neurons spike activity is a sinusoidal function of e-vector orientation with an excitatory and an inhibitory part, and with the maxima and the minima 90° apart. Thus, POL-neurons are polarisation-opponent neurons receiving input from two analyser channels with orthogonal orientations of maximal sensitivity (Labhart 1988). The two analyser channels are represented by the two sets of photoreceptors with orthogonally arranged microvilli, which are present in each ommatidium of the DRA (see Fig. 2A inset; Burghause 1979). Each POL-neuron receives antagonistic input from a large number of dorsal rim ommatidia (Helbling and Labhart 1997; T. Labhart, unpublished observations). There are three types of POL-neuron that are tuned to different e-vector orientations, about 10°, 60° and 130° with respect to the body axis (Labhart 1988; Labhart and Petzold 1993; Petzold 2000). The orientation of the ommatidia within the DRA, as defined by the transverse axis of the retinula, is variable (see Fig. 2A) and it is assumed that each tuning type of POL-neuron selectively collects input from appropriate ommatidia with more or less the same orientation. The orientations of the dorsal rim ommatidia exhibit the pattern of a distorted fan (see Fig. 2A) such that each part of the DRA contains

differently oriented ommatidia in a semicircular arrangement. Thus, each tuning type of POL-neuron could potentially receive input from ommatidia along the whole DRA. This anatomy-based assumption was confirmed by electrophysiological recordings from POL-neurons in which different parts of the DRA were selectively stimulated: Each tuning type of POL-neuron responded to exclusive stimulation of either the anterior, the middle or the posterior part of the DRA, and in each tuning type the tuning angle was the same for all three stimulus conditions (Helbling and Labhart 1996, 1997). These data are in accordance with the finding that the visual fields of the three tuning types of POL-neuron are very similar and that the tuning angle of each type is constant within the whole visual field (Petzold 2000). With a diameter of about 60° the receptive field of POL-neurons is large (Petzold 2000). Evidently, the large receptive field is a result of both optical integration at the receptor level and neuronal integration by the POL-neurons (see above). Using an opto-electronic model of a POL-neuron, the signals these large-field neurons receive from the natural polarisation pattern of the sky were studied in detail (Labhart 1999).

Let us now return to our question about the significance of the special optics in the DRA. Based on field measurements with an opto-electronic model of a POL-neuron, Labhart (1999) demonstrated that the large receptive field acts as a spatial low-pass filter, evening out local disturbances of the polarisation pattern, that are caused by clouds. This way, precise directional information can be gained from skylight polarisation even under cloudy skies (Labhart 1999). At the retina level, the small interommatidial angles, the large visual fields and the presence of retinulae with different orientations in any part of the DRA ensure that a given portion of the sky is viewed simultaneously by a large number of ommatidia containing a range of different analyser orientations. This conclusion is supported by our data on the e-vectors of maximal sensitivity $\Phi_{max}$ (see Fig. 2B). Even in cells with similar optical axes, the $\Phi_{max}$ values of R7 cells vary strongly. Thus, the cricket DRA would principally fulfill the preconditions for e-vector analysis by the "simultaneous" mechanism (Kirschfeld 1972; Edrich and von Helversen 1987), whereby the responses of the three tuning types of POL-neuron are compared to determine the e-vector (Labhart 1988). In the Canarian cricket *Cycloptiloides canariensis*, the degradation of the optics in the DRA is even stronger (Egelhaaf and Dambach 1983): apart from missing screening pigment, the DRA completely lacks corneal facetting and is devoid of crystalline cones, such that the giant rhabdoms, that are oriented approximately in parallel, must all have virtually identical and huge visual fields.

## Projections of receptor cell axons

Our data clearly corroborate the findings of Zufall et al. (1989) that the cricket DRA contains both photoreceptors with axons terminating in the lamina (SVFs) and receptors with axons projecting to the medulla (LVFs). As shown here, R7 gives rise to a LVF, whereas R1, R2, R5, and R6 have SVFs. The receptor cell recordings and markings reported by Jud and Labhart (1985) were thus probably all of the large R7 cell. R8 seems to have a LVF. However, the data for R8 are less conclusive than for the large retinula cells since they are based on retrograde labelling only. After dye application to the medulla, R8 was not marked as consistently as R7. We cannot completely exclude that R8 terminates very proximally in the lamina and may have been stained due to diffusion of dye within the optic lobe.

The microvilli of R7 (LVF) are oriented orthogonal to those of R1, R2, R5, and R6 (SVFs); the two groups of receptors represent the two analyser channels that give antagonistic input to the POL-neurons (see above). The transmitter of insect photoreceptors seems to be histamine (reviews: Nässel 1999; Stuart 1999). Specifically, using immunohistochemistry histamine was also detected in the SVFs and LVFs of the cricket DRA (Bornhauser and Meyer 1997). In all known cases, including the photoreceptor/monopolar synapse of the fly compound eye (Hardie 1989), histamine has an inhibitory action in the arthropod nervous system (Nässel 1999). The dendrites of the POL-neurons project to the dorsal rim section of the medulla (Labhart and Petzold 1993; Petzold 2000). Although not demonstrated, it is thus possible that the LVF of R7 directly connects to the POL-neuron in the medulla. Speculating that it does, R7 would represent the inhibitory analyser channel. The other receptors (with SVFs) must necessarily connect to the POL-neuron by at least one intermediate neuron, which could also serve for sign inversion to act as the excitatory channel. The results of a few pharmacological experiments are compatible with this model (H. Helbling, unpublished observations). However, a presynaptic antagonistic mechanism with the SVFs acting (inhibitory) on the LVFs in the lamina, cannot be ruled out.

The role of the short, proximal R8 is not clear. It has probably a LVF (see above) but the microvilli run orthogonal to those of the only other LVF, R7 (Burghause 1979; Labhart and Keller 1992; T. Labhart, unpublished observations). Using electron-microscopical sections at different levels along the ommatidium, we have specifically examined the ultrastructure of R8 in the DRA (T. Labhart, unpublished observations). Cell R8 seems to be a fully functional though small photoreceptor. The microvilli orientation in the small rhabdomere shows as little variation along the retinula as in the rhabdomeres of the larger cells. R8 can thus be expected to be quite strongly polarisation sensitive. On the other hand, the volume of the rhabdomere is only about 2.5% of the one of R7, or 1% of the total rhabdomere volume of R1, R2, R5 and R6. Thus, R8 is about two orders of magnitude less sensitive than any of the two putative analyser channels, and its contribution to polarisation vision can probably be neglected.

## Polarisation sensitivity

Combining intracellular recording and dye marking allowed us to discriminate between recordings from single, electrically isolated photoreceptors and multiple-cell recordings. We regard coupling between photoreceptors in the DRA of crickets as an artefact resulting from membrane damage by the electrode tip (Autrum and von Zwehl 1964) for the following reasons. (1) We found no consistent pattern of dye coupling between the different retinula cells. Coupling was either present or absent, and occurred between any neighbouring retinula cells, even between adjacent ommatidia. (2) For obvious reasons and as demonstrated in this study, coupling between photoreceptors with 90° phase-shifted e-vector response functions reduces PS, which compromises appropriate e-vector discrimination in polarisation vision. For optimal performance, the two analyser channels consisting of R7 and R1, R2, R5 and R6 (Fig. 2A inset) must be kept electrically separated before they interact antagonistically in the polarisation-opponent POL-neurons (Labhart 1988).

After sorting out the data of coupled cells, the broad distribution of PS values approached a more normal distribution (compare Figs. 4A and 4C) except for a few very large values. Exact estimates of large PS values are difficult because the receptor responses may become very small and thus noisy near the e-vector of minimum sensitivity. Using the median instead of the arithmetic mean for estimating typical PS takes care of this problem as it reduces the weight of very high and inexact values.

Since previous examinations of PS in the cricket DRA did not include dye marking, screening for single cell recordings was not possible (Gribakin and Ukhanov 1993; Labhart et al. 1984). Interestingly, median PS in these studies (6.2 and 6.5, respectively) was the same as the median calculated for our pooled single and multiple-cell recordings (6.2) suggesting similar samples (former median values are based on raw data of Labhart et al. 1984, and as read from Fig. 7 in Gribakin and Ukhanov 1993). Although Zufall et al. (1989) did mark their recordings, they did not analyse the retina for receptor cell type and multiple cell markings. In addition, their sample is small ($n = 7$) with an average PS of 6.5 (no raw data available to calculate the median).

We found no difference in PS between R7 and the cells R1, R2, R5 and R6. This is in accordance with the finding that the degree of microvillar alignment along the rhabdom is similar for all retinula cells ($\pm 9°$; Nilsson et al. 1987, and unpublished data). However, since the DRA rhabdoms are composed of two unequal microvillar blocks with a ratio of 2:1 (see Fig. 2A inset) lateral filtering might enhance PS in R7 (which forms the smaller block) relative to the other retinula cells (cf. Nilsson et al. 1987). Seemingly, this effect is impaired by the absence of screening pigment in the DRA: lateral filtering acts only on light that is guided within the rhabdoms, but much of the light absorbed by the DRA receptors is not guided (Nilsson et al. 1987). In addition, scattering effects within the pigment-free retina may also influence PS (''scattering polarizer'', see Gribakin and Ukhanov 1993). Our data give no indication for different PS classes of photoreceptors within the ommatidium (see Gribakin and Ukhanov 1993).

In conclusion, PS of photoreceptors in the DRA of crickets is typically about 10. Clearly, in order to avoid interference by coupling artefacts, screening for single-cell recordings was of utmost importance for a reliable estimate of PS.

## Conclusions

The present findings help understand some of the characteristic physiological properties of the cricket's POL-neurons. (1) The wide visual fields of the POL-neurons are a consequence of the large area covered by the photoreceptors of the DRA – both due to the large acceptance angles and the spread of the optical axes (Fig. 1B) – combined with pooling of information from a large number of photoreceptors (T. Labhart, unpublished observations). (2) All three tuning types of POL-neuron receive input from photoreceptors along the whole DRA (Helbling and Labhart 1996, 1997) and their visual fields are quite similar (Petzold 2000). These properties are based on the presence of differently oriented ommatidia in all parts of the DRA (Fig. 2A). (3) The polarisation-opponency of the POL-neurons (Labhart 1988) is reflected by the different axon projection patterns of the two photoreceptor populations that represent the two opponent analyser channels (Fig. 2A inset, Fig. 3). (4) The high e-vector selectivity of the POL-neurons – even at low degrees of polarisation (Labhart 1996) – is based on both the high PS of the photoreceptors (Fig. 4C) and the polarisation-opponent mechanism (Labhart 1988).

**Acknowledgements** Supported by the Swiss National Science Foundation. We thank Dr. Eric Warrant for critical comments on the manuscript and Kirsten Keller for expert histological work.

## References

Autrum H, Zwehl V von (1964) Die spektrale Empfindlichkeit einzelner Sehzellen des Bienenauges. Z Vergl Physiol 48: 357–384

Beersma DGM, Stavenga DG, Kuiper JW (1977) Retinal lattice, visual field and binocularities in flies: dependence on species and sex. J Comp Physiol 119: 207–220

Bornhauser BC, Meyer EP (1997) Histamine-like immunoreactivity in the visual system and brain of an orthopteran and hymenopteran insect. Cell Tissue Res 287: 211–221

Brunner D, Labhart T (1987) Behavioural evidence for polarization vision in crickets. Physiol Entomol 12: 1–10

Burghause FMHR (1979) Die strukturelle Spezialisierung des dorsalen Augenteils der Grillen (Orthoptera, Grylloidea). Zool Jahrb Physiol 83: 502–525

Edrich W, Helversen O von (1987) Polarized light orientation in honey bees: is time a component in sampling? Biol Cybern 56: 89–96

Egelhaaf A, Dambach M (1983) Giant rhabdomes in a specialized region of the compound eye of a cricket: *Cycloptiloides canariensis* (Insecta, Gryllidae). Zoomorphology 102: 65–77

Goldsmith TH, Wehner R (1977) Restrictions on rotational and translational diffusion of pigment in the membranes of a rhabdomeric photoreceptor. J Gen Physiol 70: 453–490

Gribakin FG, Ukhanov KY (1993) Effect of light scattering on visual input in arthropods. In: Wiese K, Gribakin FG, Popov AV, Renninger G (eds) Sensory systems of arthropods. Birkhäuser, Basel, pp 110–118

Hardie RC (1984) Properties of photoreceptors R7 and R8 in dorsal marginal ommatidia in the compound eyes of *Musca* and *Calliphora*. J Comp Physiol A 154: 157–165

Hardie RC (1989) A histamine-activated chloride channel in neurotransmission at a photoreceptor synapse. Nature (Lond) 339: 704–706

Helbling H, Labhart T (1996) The basis of e-vector tuning in polarization-sensitive interneurons of crickets. In: Elsner N, Schnitzler H-U (eds) Proceedings of the 24th Göttingen Neurobiology Conference. Thieme, Stuttgart, p 333

Helbling H, Labhart T (1997) Ommatidial array and e-vector tuning in polarization-sensitive interneurons of crickets. In: Elsner N, Wässle H (eds) Proceedings of the 25th Göttingen Neurobiology Conference. Thieme, Stuttgart, p 475

Herzmann D, Labhart T (1989) Spectral sensitivity and absolute threshold of polarization vision in crickets: a behavioral study. J Comp Physiol A 165: 315–319

Jud M, Labhart T (1985) The projections of the three spectral receptor types in the cricket compound eye. Experientia 41: 1221

Kirschfeld K (1969) Absorption properties of photopigments in single rods and rhabdomeres. In: Reichardt W (ed) Processing of optical data by organisms and machines. Academic Press, New York, pp 116–136

Kirschfeld K (1972) Die notwendige Anzahl von Rezeptoren zur Bestimmung der Richtung des elektrischen Vektors linear polarisierten Lichtes. Z Naturforsch 27: 578–579

Labhart T (1988) Polarization-opponent interneurons in the insect visual system. Nature (Lond) 331: 435–437

Labhart T (1996) How polarization-sensitive interneurones of crickets perform at low degrees of polarisation. J Exp Biol 199: 1467–1475

Labhart T (1999) How polarization-sensitive interneurons of crickets see the polarization pattern of the sky: a field study with an opto-electronic model neurone. J Exp Biol 202: 757–770

Labhart T, Keller K (1992) Fine structure and growth of the polarization-sensitive dorsal rim area of the compound eye of larval crickets. Naturwissenschaften 79: 527–529

Labhart T, Meyer EP (1999) Detectors for polarized skylight in insects: a survey of ommatidial specializations in the dorsal rim area of the compound eye. Microsc Res Tech (in press)

Labhart T, Petzold J (1993) Processing of polarized light information in the visual system of crickets. In: Wiese K, Gribakin FG, Popov AV, Renninger G (eds) Sensory systems of arthropods. Birkhäuser, Basel, pp 158–169

Labhart T, Hodel B, Valenzuela I (1984) The physiology of the cricket's compound eye with particular reference to the anatomically specialized dorsal rim area. J Comp Physiol A 155: 289–296

Nässel DR (1999) Histamine in the brain of insects. Microsc Res Tech 44: 121–136

Nilsson D-E, Labhart T, Meyer EP (1987) Photoreceptor design and optical properties affecting polarization sensitivity in ants and crickets. J Comp Physiol A 161: 645–658

Petzold J (2000) Polarisationsempfindliche Neuronen im Sehsystem der Feldgrille, *Gryllus campestris*. Elektrophysiologie, Anatomie und Modellrechnungen. PhD thesis, University of Zürich (in press)

Schwind R, Horváth G (1993) Reflection-polarization pattern at water surfaces and correction of a common representation of the polarization pattern of the sky. Naturwissenschaften 80: 82–83

Snyder AW (1979) Physics of vision in compound eyes. In: Autrum H (ed) Handbook of sensory physiology, vol VII/6A. Springer, Berlin Heidelberg New York, pp 225–313

Stuart AE (1999) From fruit flies to barnacles, histamine is the neurotransmitter of arthropod photoreceptors. Neuron 22: 431–433

Ukhanov KY, Leertouwer HL, Gribakin FG, Stavenga DG (1996) Dioptrics of the facet lenses in the dorsal rim area of the cricket *Gryllus bimaculatus*. J Comp Physiol A 179: 545–552

Zollikofer CPE, Wehner R, Fukishi T (1995) Optical scaling in conspecific *Cataglyphis* ants. J Exp Biol 198: 1637–1646

Zufall F, Schmitt M, Menzel R (1989) Spectral and polarized light sensitivity of photoreceptors in the compound eye of the cricket (*Gryllus bimaculatus*). J Comp Physiol A 164: 597–608